Leading edge erosion of wind turbine blades: Effects of blade surface curvature on rain droplet impingement kinematics

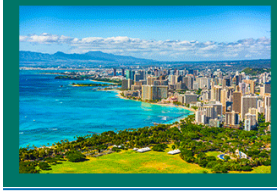

Leading edge erosion of wind turbine blades: Effects of blade surface curvature on rain droplet impingement kinematics

Amrit S. Verma[1*], Saullo G.P. Castro[1], Zhiyu Jiang[2], Weifei Hu[3], Julie J.E. Teuwen[1]

[1] Faculty of Aerospace Engineering, Department of of Aerospace Structures and Materials, TU Delft, Kluyverweg 1, 2629 HS Delft, The Netherlands
[2] Department of Engineering Sciences, University of Adger, Grimstad, Norway
[3] School of Mechanical Engineering, Zhejiang University, Hangzhou, China

E-mail: a.s.verma@tudelft.nl

Abstract. The issue of leading edge erosion (LEE) of wind turbine blades (WTBs) is a complex problem that reduces the aerodynamic efficiency of blades, and affects the overall cost of energy. Several research efforts are being made at the moment to counter erosion of WTBs such as - testing of advanced coating materials together with development of high-fidelity computational models. However, the majority of these studies assume the coated surfaces as flat, while the surface curvature and the shape of the aerofoil at the blade's leading-edge exposed to such rain fields is neglected. The present study questions the assumption of a flat surface, in the context of LEE of WTBs, and provides guidelines for erosion modelling. The critical parameters associated with rain droplet impingement kinematics on leading edge are compared for blade impact with (a) flat surface assumptions together with (b) the effects of the blade's surface curvature. A parametric study is performed which includes WTBs of varying sizes and power ratings ranging from 750 KW to 10 MW, different positions along the blade length, and different rain droplet radii ranging from 0.1 mm to 5 mm for a land based wind turbine operating at rated wind speed. It is found in the study that droplet impingement kinematics are influenced by the surface curvature at the leading edge, the effect of which is significant for representing erosion at the blade tip for smaller blades, and for exposure to rainfall intensity with larger rain droplet size. A master curve describing the threshold level along the blade length is established for various WTBs and rainfall conditions, where flat surface approximation of the surface yields noticeable error and violates the impingement process. The results of the study are expected to aid the modeller in developing advanced numerical models for LEE for WTBs.

1. Introduction

The constant demand for renewable sources of energy has led to rapid growth of large size wind turbines both in onshore and offshore sector[1]. The upscaling in the size of the turbine components poses several engineering challenges[2]. For instance, components such as wind turbine blades (WTBs) must be designed to resist complex stresses and strains during their service life [3, 4]. One of the issues related to WTBs is their leading edge erosion (LEE) which is due to the effects of harsh environmental conditions during their service life, such as repeated rain droplet impact during heavy precipitation (Fig. 1(a)). Such damages have adverse influences on their aerodynamic performance, primarily due to roughening of surfaces

Figure 1: (a) Illustration of OWT subjected to rain field [Modified picture from source: Vattenfall group[6]] (b) LEE of WTBs [7, 8][Source: TNO and DURALEDGE project]

(Fig. 1(b)), thereby contributing to substantial repair and maintenance costs. For instance, a recent study [5] showed that LEE can induce an increase in the drag coefficient by about 314%, reduction of the lift coefficient by more than 53%, together with a substantial decrease in net annual energy production of a turbine. In severe cases, damage at the leading edge can progress into the composite substrate, thereby inducing severe structural safety issues to the blades.

Given that the issue of LEE is a detrimental factor to the overall cost of energy, several research efforts are being made to control erosion of WTBs. Advanced coating materials such as leading edge protection tapes [9], protection shields [10], and elastomeric coatings [11] are being tested in rain erosion testing facilities to quantify their rain erosion resistance. It is recommended to use a coating material which has a relatively longer incubation period, thereby delaying repair and maintenance work. At the same time, emphasis is also placed on computational modelling of erosion [12, 13, 14] for understanding rain droplet impingement kinematics, kinetics as well as model damages in the blade due to rain droplet impact. Such models are expected to contribute towards enabling efficient analysis and design of coating materials for WTBs, as an alternative to costly experiments. However, the majority of the studies include performing experiments and developing numerical models by assuming the coated surfaces as flat, while the surface curvature of the blade's leading edge and the shape of the aerofoil exposed to such rain fields are neglected. In one of the rare studies, Corsini et. al [15] utilised a high fidelity computational fluid dynamics simulation to study the erosion behaviour of a 6 MW size WTB with two different blade geometries and varying aerofoil shapes. It was found in the study that the aerofoil shape significantly changes the behaviour of rain droplet impact, and exhibits varying progressive damage behaviour and erosion performance. However, the study was focused on a specific blade type, and no recommendations and comparisons were provided to specify the effects of surface curvature on the results, if the blade sections are assumed flat in the analysis.

In view of the recent studies and growing demand of developing efficient numerical models, the present study questions the assumption of a flat surface, in the context of LEE of WTBs, and provides guidelines for erosion modelling. The critical parameters associated with modelling

of rain droplet impingement kinematics on the leading edge are compared for blade impact with (a) flat surface assumptions together with the (b) effects of blade's surface curvature. A parametric study is performed which includes WTBs of varying sizes corresponding to different power ratings (750 KW to 10 MW), different positions along the blade length (blade root to tip), different rain droplet radii (0.1 mm to 5 mm) for a land-based wind turbine operating at their rated wind speeds. Finally, a master curve describing the threshold level along the blade length is established to aid the modellers, where flat surface approximation of the blade's surface yields noticeable error and violates the droplet impingement process.

The remainder of the paper proceeds as follows. Section 2 presents a brief background of the droplet impingement process and defines the scope of investigation. Section 3 presents the problem statement and discusses the details of the parametric study considered in this work. Section 4 discusses important results with context to effect of surface curvature on LEE of WTBs. Finally, section 5 concludes the paper along with recommendations for future work.

2. Background

In this section, a brief background summarising different phases of high speed rain droplet impingement on a solid surface, along with different erosion mechanisms are presented. A description of important parameters associated with initial compressible stage of liquid impingement is presented along with governing equations and underlying key assumptions for flat and curved surfaces based on models from Adler et al. [16] and Thomas et al. [17] respectively.

2.1. Phases of high speed rain droplet impingement

There are two distinct phases for a case where a high speed water droplet, typically above 50 m/s, impinges on a blade solid surface (Fig. 2(a)). The details of these phases are comprehensively described in [18, 19, 20] and are discussed briefly below.

A. Initial compressible phase: This stage represents the phase of initial contact between the liquid and the solid surface, where a zone of compressed liquid is formed at the contact zone between the droplet and the solid surface (Fig. 2(b)). During this stage, the rate at which the contact periphery between the droplet and solid surface increases is larger than the rate at which the impact-induced shock waves propagate within the liquid droplet. As a result, at this stage, the rest of the liquid outside the compressed zone, is incognizant of the impingement process with the solid surface. The region between the compressed and the incognizant liquid is disjointed by a shock front, which is attached to the contact surface at this stage. Also, a very high impact pressure, in the order of few hundreds MPas, are generated on the solid surface over a very small contact duration, which is in the range of a few μs. This pressure is also regarded as water hammer pressure (P_{wh}) in the literature [21], and is given by:

$$P_{wh} = \rho_l C_l V \tag{1}$$

where ρ_l is the density of water ($1000 kg/m^3$), V is the velocity of impact and C_l is the shock velocity in liquid droplet given by:

$$C_l = C_o + \nu V \tag{2}$$

where ν is a constant considered as 2 for water, and C_o is the speed of sound in water and is taken as 1500 m/s [21]. The above equation is valid for rigid solid surface, and if the compliance of the impacted surface is taken into account, then the water hammer pressure is given as:

$$P_{wh} = \frac{\rho_l C_l V_{imp}}{1 + \dfrac{\rho_l C_l}{\rho_s C_s}} \tag{3}$$

where ρ_s and C_s are density of and speed of sound in the coating material respectively.

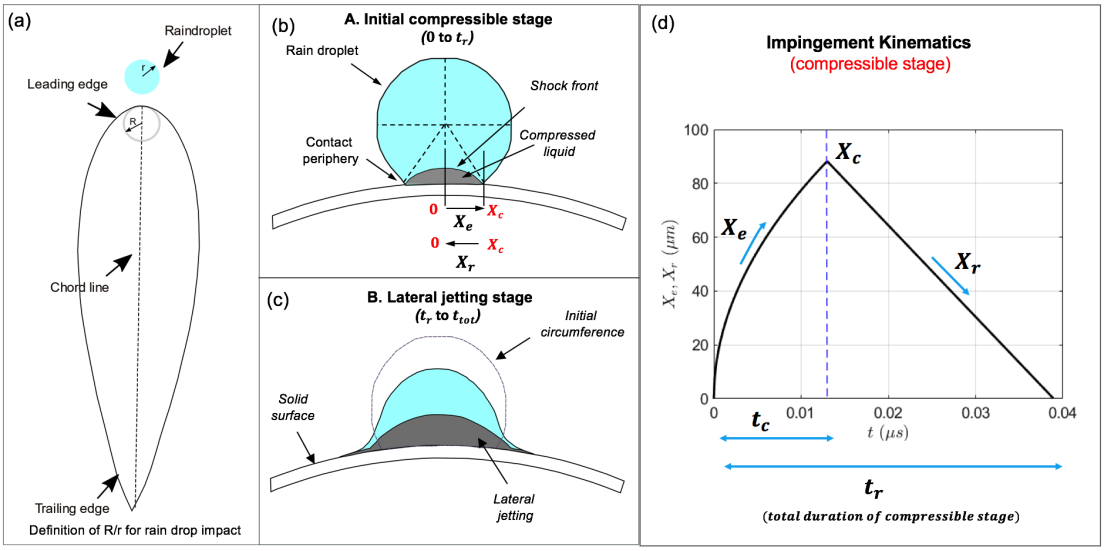

Figure 2: (a) Rain droplet impact on blade's leading edge (b) Initial compressible stage (c) Lateral jetting stage (d) Description of parameters for droplet impingement kinematics

B. Lateral jetting stage: This stage represents the phase of droplet impact where the shock front overtakes the contact radius (Fig. 2(c)). The high pressure developed during the compressible stage is released, causing a significant reduction in the pressure. As a result, there is a high velocity flow of the liquid in the radial direction of the droplet impact. This velocity of the liquid flowing in the radial direction during the lateral jetting stage is found in the literature [22] in the order of 3 to 10 times the initial impingement velocity of the droplet.

2.2. Scope of investigation

Due to the above stated phases described for high speed water droplet impact, there could be four progressive means through which the erosion damage can occur in the solid surface in the course of repetitive exposure - (1) Direct deformation (2) Stress wave propagation (3) Lateral jetting effects, and (4) Hydraulic penetration [22]. The direct deformation mechanism, and stress wave propagation are associated with initial compressible stage, and are related to initiation of damage, such as local pitting, due to high water hammer pressure. On the other hand, lateral jetting and hydraulic penetration require an existing damage in material and act as crack propagators, inducing material removal due to high shear stresses and stress concentrations. Most of the design aspects for a material resistance against droplet impact erosion focus on the first two aspects - direct deformation mechanism and stress wave propagation contributed during compressible stage, given that the material still has sufficient erosion capacity. In addition, the initiation of cracks and material removal is delayed, making coating more erosion resistant. As a result, 'initial compressible stage' is an important phase considered for analysis of coating for LEE. In the current study, the investigation is restricted to this stage, and important parameters describing this stage are discussed below.

2.3. Description of droplet impingement parameters:

The pressure developed during the compressible stage can be distinguished to act into different sub-phases (Fig. 2(d)). The first sub-phase corresponds to the time period between 0 to t_c, where the contact area is expanding with a radius of X_e (Fig. 2(d)). Once the shock front advances the contact periphery, this is the time (t_c) when maximum contact radius (X_c) is

Table 1. Droplet impingement kinematics for flat surfaces [16] and curved surfaces [17]

Parameter	Description	Flat surface [16]	Curvature effects [17]
X_e	Contact radius during expansion	$\sqrt{[2rVt-(Vt)^2}$	$\sqrt{R^2-\frac{[(R+r-Vt)^2+(R^2-r^2)]^2}{4(R+r-Vt)^2}}$
X_c	Maximum contact radius	$\frac{Vr}{C_l}$	$C_l=\frac{V[(R+r-Vt)^4-(R^2-r^2)^2]}{4X_e(1-(X_e/r)^2)^{1/2}(R+r-Vt)^3}$
t_c	Time when the shock front overtakes the contact periphery	$\frac{r}{V}\left(1-\sqrt{1-(1-\left(\frac{V^2}{C_l^2}\right)}\right)$	$X_e(1-\frac{X_e^2}{r^2})^{1/2}-\frac{V[(R+r-Vt)^4-(R^2-r^2)^2]}{4C_l(R+r-Vt)^3}=0$ (Numerical solution to the above equation yields t_c, which can be substituted in X_e to obtain X_c)
X_r	Contact radius during contraction	$X_c-C_l(t-t_c)$	$R\sin\left(sin^{-1}\left(\frac{X_c}{R}\right)-\frac{C_l}{R}(t-t_c)\right)$
t_r	Total duration of compressible stage	$\frac{3rV}{2C_l^2}$	$t_c+\frac{R}{C_l}sin^{-1}\left(\frac{X_c}{R}\right)$

R: Leading edge radius | r: Rain droplet radius | V: Impact velocity normal to blade surface | t: Time from impingement initiation

achieved. The second sub-phase corresponds to the time period between t_c and t_r, where the contact area is contracting with a radius of X_r, due to release waves traversing from the contact periphery towards the central axis. $t = t_r$ marks the end of compressible stage of droplet impact. The formulations used in this study are based on the model from Adler et al.[16] for flat surface, and Thomas et al.[17] for curved surfaces, which are also tabulated in Table 1. The details of how these parameters were derived can be found in [16, 17]. Note that Thomas et al.[17] reformulated the governing equations of [16] by including a variable R for radius of the solid surface, also referred as leading edge radius in this paper. Further the results were qualitatively validated with experiments [22] where high speed water droplet impact on aeroengine fan blades with different R were investigated. However, it is to be noted that the analysis and validation of theoretical predictions in [17, 22] were made for a droplet impact speed in the range 200-400 m/s, which corresponds to impact conditions for aeroengine fan blades. In the current study, impact speed is less than 150 m/s, which is a typical range of blade tip speed for existing WTBs.

2.4. Key assumptions:

The key assumptions included in the derivation of the impingement models described above [16, 17] are:

1. The rain droplet is considered spherical in shape in both the models.
2. The models treat the 3D rain droplets as a two-dimensional approximation.
3. In the model from [17], it is assumed that the plane of cross-section of spherical rain droplet is parallel to the circular face of the target body, given that the effect of curvature on the droplet impingement will be most pronounced.
4. The target body is assumed free of imperfection with no initial surface roughness and pre-existing cracks.
5. The effects of droplet impingement angles are ignored in both the models, and the droplet impact is assumed normal to the surface.

3. Problem statement and details of parametric study

The primary variable for rain droplet impingement on a blade surface is the ratio between leading edge radius (R) and impacting radius of rain droplet (r) (Fig. 2(a)). Typically, flat surface

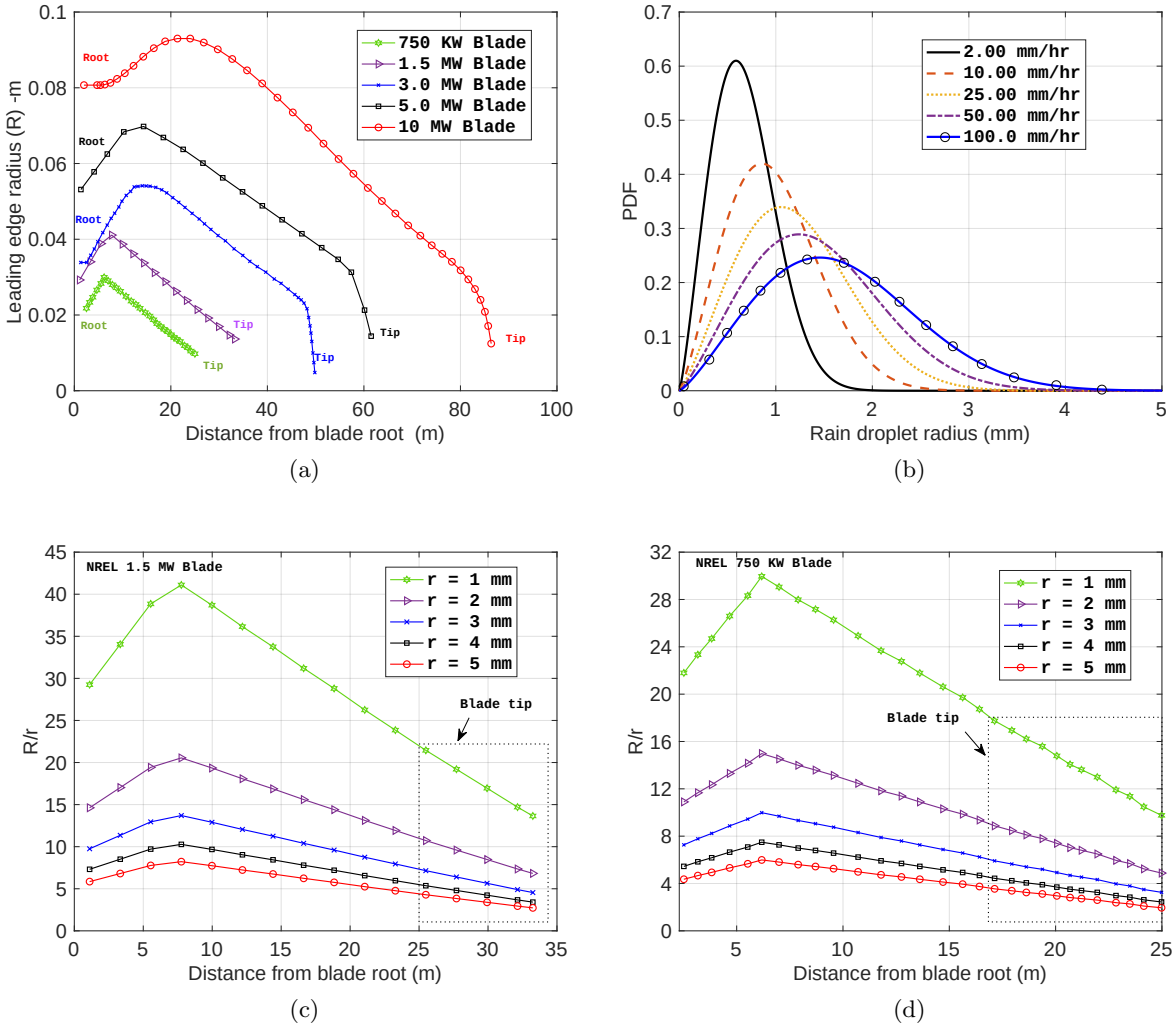

Figure 3: (a) R for WTBs for different power ratings [23, 24] (b) Probability density function (PDF) of r varying with I [25]; R/r for WTBs for (c) NREL 1.5 MW turbine [26] (d) NREL 750 KW turbine[26]

approximation is considered as a reasonable assumption when the ratio R/r is sufficiently large (such as for the case of steam turbine blades and surfaces of aircraft)[17]. However, as R/r reduces, the effect of curvature is expected to have a significant influence on the erosion process. Nevertheless, it is still not quantitatively clear what the threshold range of R/r is, where the flat surface is a sound assumption, and where such an assumption violates the impingement process, especially when applied to rain droplet impact on a WTB.

For a generic aeroengine fan blade, the threshold value of R/r has been found to be around 10, for a case with droplet impact speed in the range of 200-400 m/s [17]. However, when it comes to a WTB, 'R' changes continuously from root to tip depending upon its chord length distribution and power rating, and sections along the blade length are exposed to varying impact speeds. For instance, variations in the R from blade root to tip are compared for WTBs corresponding to different turbines' power ratings ranging from 750 KW to 10 MW in Fig. 3(a). The leading edge radius (R) for WTBs is assumed as 1% of the chord length in this study, however, it is to

be noted that this geometrical characteristics is also dependent on the thickness of the chord [27]. It can be seen that typical R values increase from root towards the blade tip, and can range from 80 mm at the root for 10 MW blade to less than 5-10 mm near the blade tip for a 750 KW blade. In addition, given that the rain droplet radius (r) can vary between 0.1 mm to 5 mm (Fig. 3(b)) depending upon the rainfall intensity (I) and droplet size distribution (DSD)[28], a considerable variation in the ratio of R/r can be seen along the blade length for different rainfall conditions. Fig. 3b is produced using the Best's droplet size distribution (DSD) [25], which provides probability distribution of rain droplet size (ϕ_d: droplet diameter) for given rainfall intensity, which is given by:

$$F(\phi_d) = 1 - exp\left(\frac{\phi_d}{1.3 * I^{0.232}}\right)^{2.25} \tag{4}$$

For instance, variations of R/r varying from blade root to tip for different sections along the blade length for NREL 1.5 MW blade and NREL 750 KW blade are presented in Figs. 3(c) and 3(d) respectively. It can be seen that the ratio R/r values vary considerably along the blade length, and reduce notably at the blade tip for all the cases. Therefore, in the current study, an attempt is made to investigate the threshold position along the blade length, till where the flat surface assumption is valid for modelling raindrop impingement process. As described earlier, a parametric study is performed to include different WTBs, different positions along the blade length, and different rain droplet radii (0.1 mm to 5 mm) for a land-based wind turbine and operating at rated wind speeds.

4. Results

In this section, parameters for rain droplet impingement kinematics on a solid surface describing the droplet compressible stage, for various R, r and V are discussed. Further, the results for the parametric study are presented. Comparisons are made between results for flat surface approximations and surface curvature formulations, and modelling guidelines are presented for different WTBs, different rainfall conditions and various positions along the blade length.

Fig. 4(a) compares the droplet impingement on solid surfaces with varying radii of curvature ($R = \infty, 100\ mm, 50\ mm, 10\ mm, 1\ mm$), impacted by a droplet with a radius $r = 1\ mm$ and having impact velocity $V = 100\ m/s$. The rate of increase in the contact radius (X_e) between droplet and solid surface upon impact increases with increasing values of R, with results using flat surfaces closely matching with surfaces having larger radii of curvature ($R = 100\ mm, 50\ mm$). However, with smaller values of R ($R = 1mm$), the differences in the estimates for X_e and maximum contact radius (X_c) between droplet and solid surface, analysed without considering surface curvature, are overestimated by more than 40%. Further, this difference is significant with a larger rain droplet radius ($r = 5mm$), as shown in Fig. 4(b), where estimates for X_e and X_c using flat surface solutions are overestimated by 5-6 times for a case with $R = 1\ mm$. Also, the time when the shock-wave overtakes the contact radius (t_c) and the total duration of compressible stage (t_r) reduces with decreasing values of R, which implies early commencement of lateral jetting stage for smaller values of R; this is expected to induce accelerated material removal and higher rate of erosion. As a result, estimates using flat surface formulations can underestimate the erosion of blades, especially for smaller R (close to the blade tip), and larger r's representing exposure to high rainfall intensity (I). However, no differences in values of X_r are found due to droplet impact, as their slope (from t_c to t_r) is consistent for all the cases. Further, the effects of r and V on the rain droplet impingement on solid surface with a constant R is shown in figs. 4(c) and 4(d) respectively, where parameters such as X_e, X_c, t_c, and t_r are found to increase with increasing r and increasing V. However, larger changes in these values are obtained with changing values of r, compared to changes in values of V, which implies the importance of a large droplet size during blade erosion.

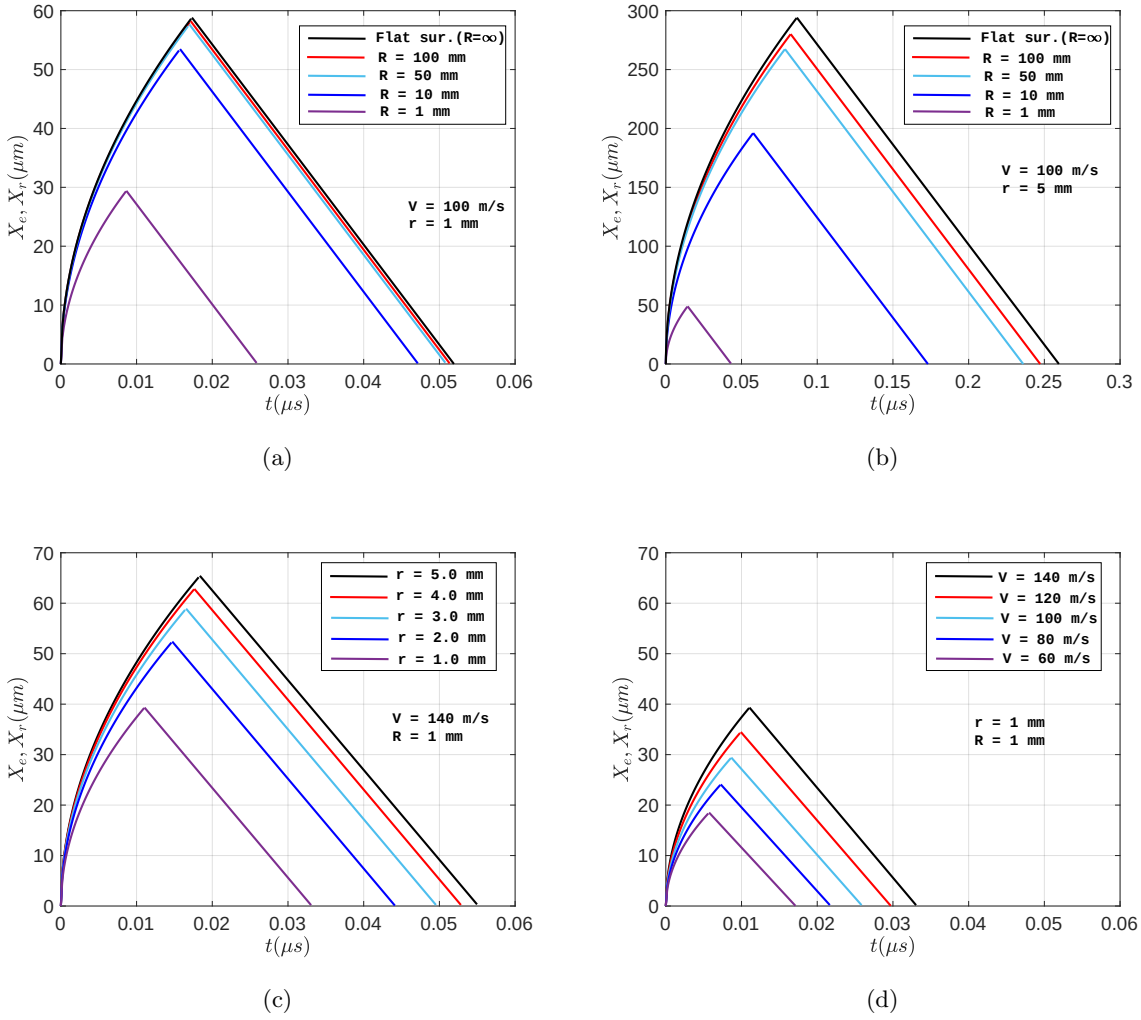

Figure 4: Droplet impingement kinematics for $R = \infty, 100, 50, 10, 1\ mm$, $V = 100\ m/s$ (a) $r = 1\ mm$ (b) $r = 5\ mm$ (c) $r = 1, 2, 3, 4, 5\ mm$, $V = 140\ m/s$(d) $V = 60, 80, 100, 120, 140\ m/s$

Figs. 5(a)-(d) compare the estimated t_c using flat (F) and curved surface (C) formulations for droplet impingement on leading edge surfaces corresponding to different WTBs and power ratings (750 KW to 10 MW) and at different positions along the blade length, impacted by rain droplet with radii ($r = 0.5\ mm, 2.0\ mm, 4.0\ mm$). All the results represent WTBs rotating at their respective rated rotor speeds. It can be seen from these figures that the flat surface approximation over-predicts t_c for all the cases, the effect of which is major for larger rain droplet sizes and smaller WTBs. These values tend to deviate more towards the blade tips, which implies the importance of surface curvature to be included in the modelling of LEE especially at the blade tip. Also, the difference in the values of t_c estimated using flat (F) and curved surface (C) formulations, are quite significant along the entire blade length, especially for smaller blades having smaller values of R - NREL 750 KW blade (24 m), and NREL 1.5 MW blade (35 m), and for case with $r = 4\ mm$. Similar observations can be seen in the results for the maximum contact radius (X_c) obtained between droplet and solid surface using flat (F) and curved surface (C) formulations, as shown in Figs. 6(a)-6(d). Like t_c, X_c is also overestimated when the effects

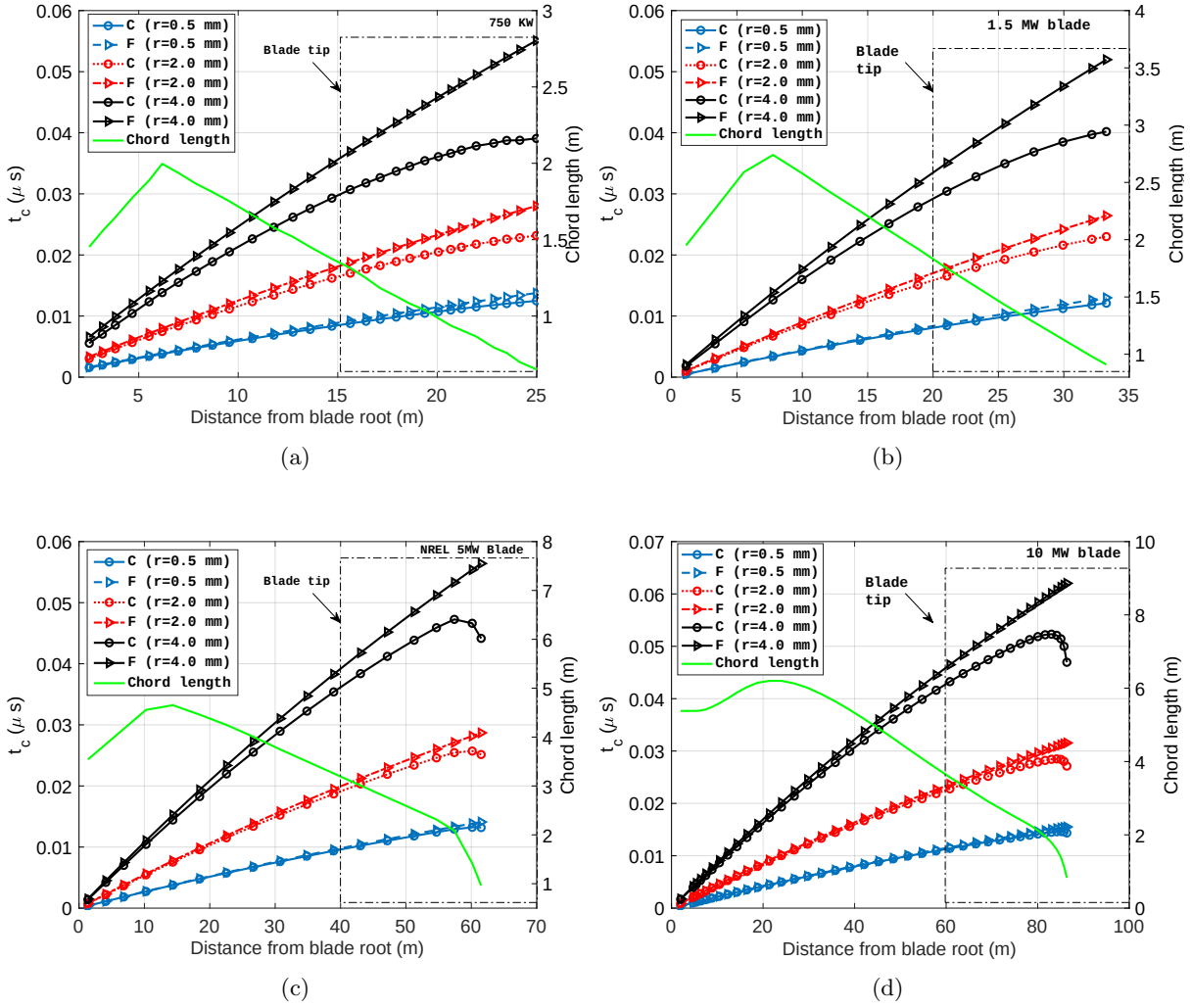

Figure 5: Comparison of t_c estimated from flat (F) and curved surfaces (C) for (a) NREL 750 KW (b) NREL 1.5 MW (c) NREL 5MW (d) DTU 10 MW blade and $r = 0.5\ mm, 2\ mm, 4\ mm$

of surface curvature are not included in erosion modelling, and blade surfaces are modelled as flat. The differences are most significant at the blade tip for all the blade lengths, and significant for larger values of rain droplet size. Again, as observed before, the differences are significant for smaller blades compared to large size WTBs, as seen while comparing t_c between 750 KW blade and 10 MW blade.

From the above discussions, it is clear that different combinations of rainfall conditions and blade types with varying blade lengths and chord distributions will have different thresholds along the blade length, where results from flat surface approximation violates the impingement process. In order to establish a master curve, where flat surface approximation of the surface yields noticeable error and violates the impingement process, a normalized parameter $\overline{t_r}$ is introduced. $\overline{t_r}$ is defined as the ratio between t_r estimated using curved formulations and t_r obtained using flat surface solutions. A difference of more than 10% in the value ($t_r \leq 0.9$) is defined as the threshold where flat surface approximation of the surface yields noticeable error [17], and requires surface curvature to be included for LEE modelling of WTBs.

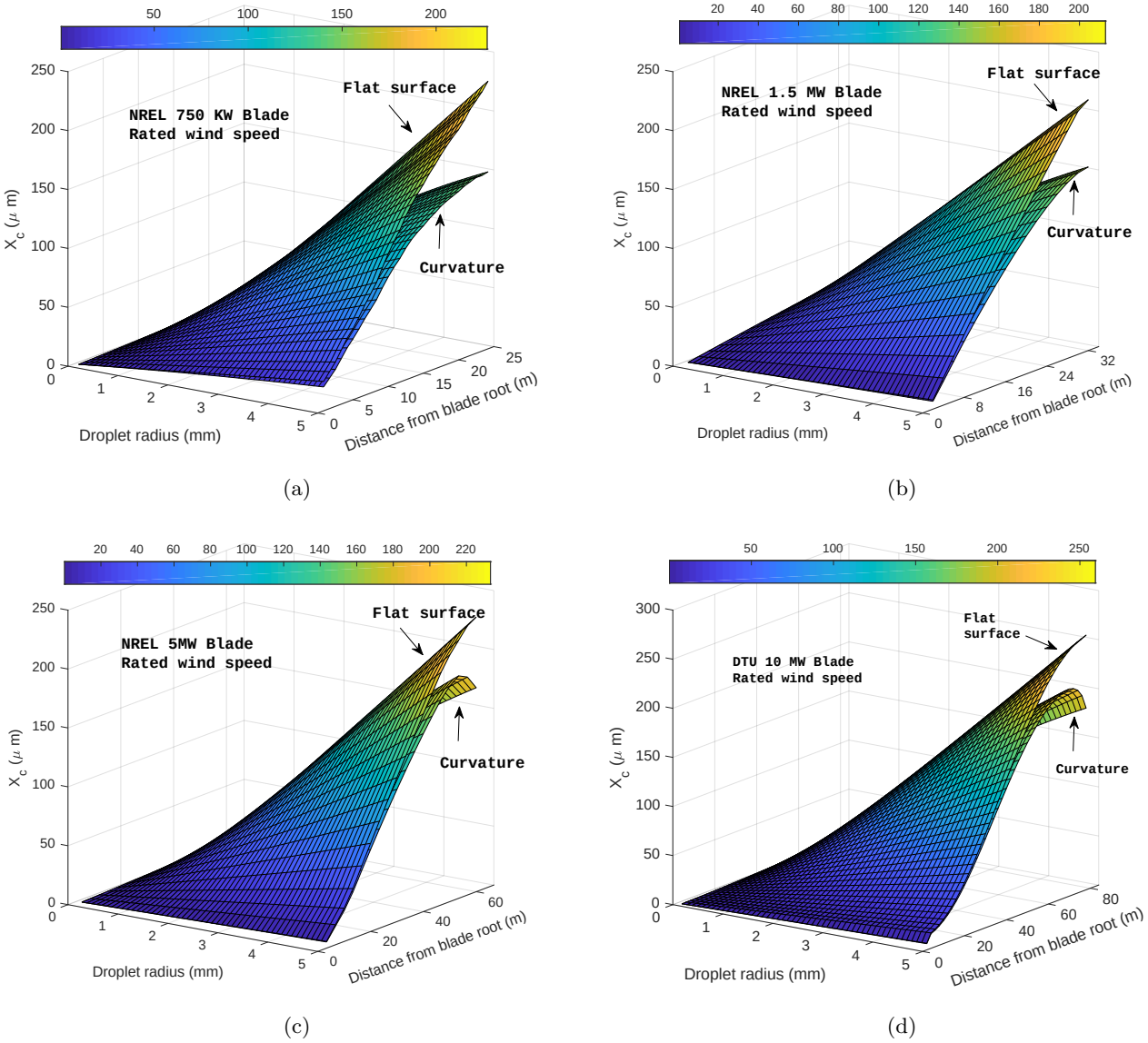

Figure 6: Comparison between X_c estimated from flat and curved surfaces for (a) NREL 750 KW (b) NREL 1.5 MW (c) NREL 5 MW (d) DTU 10 MW blade and different r

Figs. 7(a)-(d) show the master curve where $\overline{t_r}$ is presented for droplet impingement on the leading edge surface at different positions along the blade length from the blade root (d) which is normalized with the total blade length(L). The figures represent different WTBs of varying power ratings ranging from 750 KW to 10 MW, and impacted by rain droplets having radii $r = 0.5\ mm, 1\ mm, 2\ mm, 3\ mm, 4\ mm$, and $5\ mm$. All points lying below the black dotted line (90% line) in all the figures imply an error of at least 10% in modelling rain droplet impingement kinematics for WTBs, if surfaces are modelled as flat. As expected, the error is found largest at the blade tip for all the cases, and increases with increasing rain droplet size. Also, for smaller WTBs (NREL 750 KW and NREL 1.5 MW) and with moderate values of rain droplet size, large percentage of sections along the blade length are found to lie below the threshold line, thereby implying absolute requirement of blade's surface curvature to be included in the

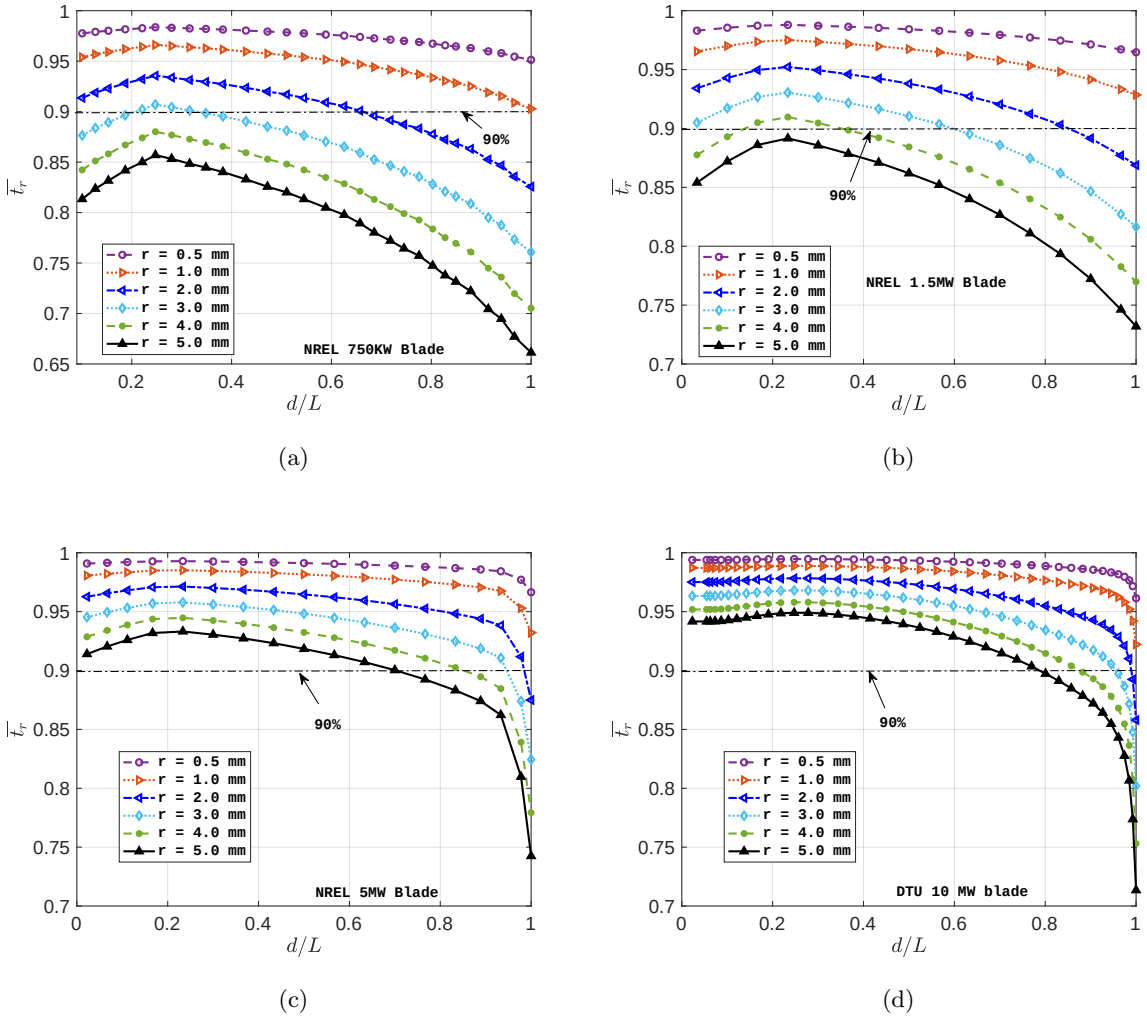

Figure 7: $\overline{t_r}$ for (a) NREL 750 KW (b) NREL 1.5 MW (c) NREL 5MW (d) DTU 10 MW blade

erosion modelling while dealing with small size WTBs. For instance, for 750 KW blade, any impingement process that includes droplet size above $r > 2-3\ mm$, will yield an error in the range of 20%-35% if the sections ($d/L \geq 0.6$) are modelled as flat in the analysis. On the other hand, for large size WTBs representing turbines with higher power ratings (NREL 5 MW and DTU 10 MW), the error is mostly pronounced very close to the blade tip ($d/L \geq 0.85$), and yields noticeable error for values of very large droplet sizes which is relevant for high intensity rainfall conditions.

5. Conclusion and recommendations for future work

The present study questions the assumption of a flat surface, in the context of LEE of WTBs, and provides guidelines for erosion modelling. It is found in the study that droplet impingement kinematics are influenced by the surface curvature at the leading edge, the effect of which is significant for representing erosion at the blade tip for smaller blades, and for exposure to rainfall intensity with larger rain droplet size. A master curve describing the threshold level along the blade length is established for various WTBs and rainfall conditions, where flat surface

approximation of the surface yields noticeable error and violates the impingement process. The current study is limited to understanding the mechanism of single rain droplet impact on the leading edge emphasising explicitly on the droplet compressible stage. However, a detailed understanding of stresses and possible differences in the damage modes, that could develop on the coating surface for such scenarios, were not considered or modelled. A numerical study based on finite element analysis will be carried out in the future with different R/r ratios and coating properties to evaluate how the stresses and impact pressures vary with the effects of surface curvature and influence the results. Also, in all the cases, it is assumed that the rain droplet impacts in the normal direction to the blade's surface. In the future, existing erosion models will be improved by including the effects of droplet impingement angles.

6. Acknowledgement

This work was made possible through the WINDCORE project having subsidy scheme TSE-18-04-01-Renewable energy project with project number TEHE1180113.

References

[1] Verma A S, Jiang Z, Ren Z, Gao Z and Vedvik N P 2019 *Energies* **12** 1867
[2] Verma A S, Jiang Z, Gao Z and Vedvik N P 2020 *Marine Structures* **72** 102778
[3] Pugh K, Rasool G and Stack M M 2019 *Journal of Bio-and Tribo-Corrosion* **5** 45
[4] Verma A S, Jiang Z, Vedvik N P, Gao Z and Ren Z 2019 *Engineering Structures* **180** 205–222
[5] Han W, Kim J and Kim B 2018 *Renewable energy* **115** 817–823
[6] Picture taken under permission from Vattenfall group, https://group.vattenfall.com/what-we-do/our-energy-sources/wind-power
[7] Picture taken under permission from TNO, https://www.tno.nl
[8] Picture taken under permission from DURALEDGE Project, http://www.duraledge.dk
[9] https://www.3m.com
[10] Chen J, Wang J and Ni A 2019 *Journal of Coatings Technology and Research* **16** 15–24
[11] Slot H, Ijzerman R, le Feber M, Nord-Varhaug K and van der Heide E 2018 *Wear* **414** 234–242
[12] Verma A S, Castro S G, Jiang Z and Teuwen J J 2020 *Composite Structures* 112096
[13] Keegan M H, Nash D and Stack M 2012 *ASME Turbo Expo 2012* Article–GT
[14] Amirzadeh B, Louhghalam A, Raessi M and Tootkaboni M 2017 *Journal of Wind Engineering and Industrial Aerodynamics* **163** 33–43
[15] Corsini A, Castorrini A, Morei E, Rispoli F, Sciulli F and Venturini P 2015 *ASME Paper No. GT2015-42174*
[16] Adler W 1979 The mechanisms of liquid impact, treatise on materials science and technology," vol. 16, erosion, carolyn m. preece, ed
[17] Burson-Thomas C B, Wellman R, Harvey T J and Wood R J 2019 *Journal of Engineering for Gas Turbines and Power* **141** 031005
[18] Sareen A, Sapre C A and Selig M S 2014 *Wind Energy* **17** 1531–1542
[19] Engel O G 1973 *Journal of Applied Physics* **44** 692–704
[20] Blau P J 1992 *ASM Handbook, Volume 18-Friction, Lubrication, and Wear Technology* (ASM international)
[21] Slot H, Gelinck E, Rentrop C and Van Der Heide E 2015 *Renewable Energy* **80** 837–848
[22] Burson-Thomas C B, Wellman R, Harvey T J and Wood R J 2019 *Wear* **426** 507–517
[23] Bak C, Zahle F, Bitsche R, Kim T, Yde A, Henriksen L C, Hansen M H, Blasques J P A A, Gaunaa M and Natarajan A 2013 *Danish Wind Power Research 2013*
[24] Jonkman J, Butterfield S, Musial W and Scott G 2009 *National Renewable Energy Laboratory, Golden, CO, Technical Report No. NREL/TP-500-38060*
[25] Best A 1950 *Quarterly Journal of the Royal Meteorological Society* **76** 16–36
[26] Dykes K L and Rinker J 2018 Windpact reference wind turbines Tech. rep. National Renewable Energy Lab.(NREL), Golden, CO (United States)
[27] Kerwin J E 2001 13.04 lecture notes hydrofoils and propellers
[28] Verma A S, Jiang Z, Zhengru R and Teuwen J J 2020 *39th International Conference on Ocean, Offshore and Arctic Engineering OMAE (2020)*